Hydrodynamic and Chemical Modeling of a Chemical Vapor Deposition Reactor for Zirconia Deposition

T. Belmonte, J. Gavillet, T. Czerwiec, D. Ablitzer, H. Michel

Hydrodynamic and Chemical Modeling of a Chemical Vapor Deposition Reactor for Zirconia Deposition

T. Belmonte (*), J. Gavillet, T. Czerwiec, D. Ablitzer and H. Michel

Laboratoire de Science et Génie des Surfaces (**), École des Mines de Nancy, Institut National Polytechnique de Lorraine, Parc de Saurupt, 54042 Nancy Cedex, France

(Received 12 November 1996, revised 25 February 1997, accepted 7 May 1997)

PACS.81 15.Gh – Chemical Vapor Deposition (including plasma-enhanced CVD, MOCVD, *etc.*)

PACS.47 70.Fw – Chemically reactive flows

PACS.82.20.Pm – Rate constants, reaction cross sections, and activation energies

Abstract. — Zirconia is deposited on cylindrical substrates by flowing post-discharge enhanced chemical vapor deposition In this paper, a two dimensional hydrodynamic and chemical modeling of the reactor is described for given plasma characteristics. It helps in determining rate constants of the synthesis reaction of zirconia in gas phase and on the substrate which is $ZrCl_4$ hydrolysis. Calculated deposition rate profiles are obtained by modeling under various conditions and fits with a satisfying accuracy the experimental results. The role of transport processes and the mixing conditions of excited gases with remaining ones are studied. Gas phase reaction influence on the growth rate is also discussed.

Nomenclature

C_p	specific heat at constant pressure (J kg^{-1} K^{-1})	M	molar weight (kg mol^{-1})
D	diffusion coefficient (m^2 s^{-1})	P	pressure (Pa) or perimeter (m)
$\mathbf{g}$	gravitation field (m s^{-2})	S_T	heat sources (J m^{-3} s^{-1})
h	heat transfer coefficient (W m^{-2} K^{-1})	$S_{\omega i}$	consumption source of the reactive species i (kg m^{-3} s^{-1})
k	thermal conductivity (W m^{-1} K^{-1})	T	temperature (K)
$k_{s,v}$	rate constants for surface or gas phase reaction (m^6 kg^{-2} s^{-1})	T_m	averaged temperature (K)
		T_w	wall temperature (K)
		$\mathbf{v}$	fluid velocity (m s^{-1})

(*) Author for correspondence (e-mail: belmonte@mines.u-nancy.fr).
(**) URA CNRS 1402

Dimensionless Numbers

Gr	Grashof
Kn	Knudsen
Nu	Nusselt
Re	Reynolds

Greek Letter

ρ	fluid density (kg m^{-3})
$\overline{\overline{\tau}}$	stress tensor (N m^{-2})
ω_i	mass fraction (kg kg^{-1})

Notation

$\sim$	dimensionless variable
subscript	
c	cold wall
h	hot wall
g	overall
s	surface
v	volume
A	$ZrCl_4$
B	H_2O
F	ZrO_2

1. Introduction

Flowing post-discharge (also called Remote Plasma) Enhanced Chemical Vapor Deposition (RPECVD) is finding increasing applications [1–5]. Indeed, low temperatures (from 573 K to 753 K) allow the use of substrates such as polymers or metallic alloys which are treated thermally or thermo-chemically and whose structures can be damaged by high temperatures. Removal of the substrate from the plasma environment reduces surface damage by suppressing energetic ions bombardment and photons exposure [6, 7].

In typical RPECVD reactors, a gas mixture is passed through a discharge and brought into contact where the substrate is located with a second unexcited gas mixture introduced upstream. Only neutral species of the plasma are transported to the processing chamber where deposition takes place. Therefore, reaction pathways in RPECVD systems are more constrained than those in direct PECVD [2].

In this paper, RPECVD of zirconia in late post-discharge is considered. ZrO_2 has low electric conductivity and extreme chemical inertness. ZrO_2 is suitable for applications in semiconductor devices [8], thermal barrier coatings [9], or oxidation resistance coatings [10].

ZrO_2 was deposited by reaction between $ZrCl_4$ and a late O_2-H_2-Ar post-discharge. The use of late post-discharges was initially to synthesise thin films on long substrates. Plasma assistance was chosen because oxidation of $ZrCl_4$ by O_2 was impossible and assumed to be very difficult by water [11]

Indeed, before our work, no result was available in the literature on $ZrCl_4$ hydrolysis between 573 K and 753 K for this reason that handling water was described to lead to unsuitable results [11]. In a previous paper [12], a complete characterization of the late post-discharge was carried out. Water presence was observed in the late post-discharge with no doubts. A comparison was drawn between the RPECVD process and the hydrolysis of $ZrCl_4$ by conventional CVD. In the temperature range [573 K–753 K], the reaction pathway for zirconia deposition was demonstrated to be the hydrolysis of the zirconium tetrachloride The use of a plasma in this

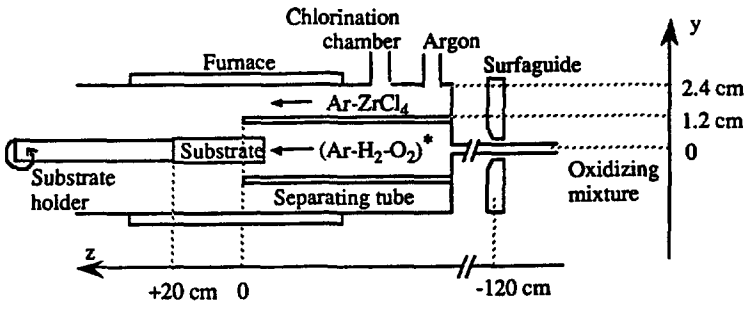

Fig. 1. — Experimental device.

case was a very simple mean to determine a partial pressure of water at the inlet of the reaction zone. It was concluded that our RPECVD process was, in the late post-discharge and in the range of temperature given above, comparable with a conventional hydrolysis process.

The main result of the previous study [12] was that water could be handled without stringent precautions but in conditions that could not be found easily without the use of a post-discharge. According to authors' knowledge, nothing is available on $ZrCl_4$ hydrolysis in the range of temperature from 573 K to 753 K. Our step was the only mean to demonstrate that the use of low partial pressures of water in very precise hydrodynamic conditions enable zirconia synthesis below 1223 K.

The purpose of this work is first to explain, by a transport and chemical approach, the reason why water can be handled so easily in our conditions, whereas it is explained that it was a problem in all the previous studies. For that, the rate constant for $ZrCl_4$ hydrolysis reaction in the gas phase and on the substrate will be proposed. A complete description of the reactor was the only mean to determine these values. The influence of the process parameters on deposition rate is also used to validate the calculated rate constants. From then on, calculations are performed at higher temperature to explain what was observed by other authors.

The second purpose of this work is also to examine transport phenomena in a CVD reactor with a process approach in order to control film synthesis. This is an important step in the optimization scheme of our process. The thickness homogeneity of layers is improved to lead to weakly decreasing deposition rates along the substrate. The modeling also helps us to understand why the experimental conditions leading to zirconia formation at low temperature could not be easily found with conventional CVD approaches.

2. Experimental Apparatus

The RPECVD apparatus consists of three parts : 1) the microwave excitation of an $Ar-O_2-H_2$ mixture; 2) a chlorination chamber to perform $ZrCl_4$ *in situ* synthesis and 3) the furnace where the substrate is located (Fig. 1). The transport of the excited species to the substrate is ensured by a tube which also separates them from other gases.

The plasma source is produced in a quartz tube (5 mm inner diameter) by a 2.45 GHz microwave system with a surfaguide surface wave launcher located upstream (1.2 m) from the deposition chamber. Delivered power is constant (130 W).

To avoid gas phase reactions, the oxidizing mixture flows through the discharge and reaches the reaction zone in a quartz tube (15 mm inner diameter) separating this oxidizing mixtures

Table I. — *Reference conditions.*

General conditions
$T = 753$ K
$P = 15$ hPa
Substrate location: 3 cm inside the separating tube
Discharge parameters
$P_w = 130$ W
$Q_{Ar} = 1027$ sccm
$Q_{O_2} = 12.5$ sccm
$Q_{H_2} = 24.5$ sccm
H_2O partial pressure at $z = 0$: 22 5 Pa
$Q_{H_2O} = 15$ sccm
Chlorination conditions
$T = 623$ K
$Q_{Ar} = 21$ sccm
$Q_{Cl_2} = 5$ sccm

from the $Ar-ZrCl_4$ mixture. Typical gas flow rates are indicated in Table I. Each species except argon can then be considered as very diluted.

The chlorination chamber is an *in situ* synthesis device of $ZrCl_4$ from an $Ar-Cl_2$ mixture flowing through a zirconium bed heated to 623 K. The reaction $Ar+Cl_2 \rightarrow ZrCl_4$ is complete under these conditions of temperature and pressure, what is verified by mass loss measurements. Argon flow rate is 21 sccm while Cl_2 is in the [0-5 sccm] range.

The substrate is located 1.20 m downstream from the gap discharge, in a furnace with an isothermal zone of 30 cm. Temperature is chosen equal to 623 K or 753 K. The substrate is a cylinder (9.5 mm outer diameter) of 20 cm length. A holder, with the same cylinder shape, penetrates and supports the substrate. It rotates to ensure a constant radial deposition rate distribution. Rotation is considered low enough (actually 0.6 rad s^{-1}) to ignore any possible pressure diffusion effect. Therefore, $ZrCl_4$ distribution is assumed to be cylindrical. The reactor is a quartz tube (inner diameter of 28 mm). Two geometrical configurations are studied according as the substrate is entered into the separating tube or remains outside a distance of 3 cm.

3. Experimental Results

Experiments are carried out at 623 K and 753 K in the conditions specified in Table I. The deposition rates are calculated from SEM micrographs. The substrate, after treatment, is sawed in pieces of one centimeter long, and submitted to a mechanical strain till the layer broke. These results will be compared hereafter with calculated deposition rates.

For a given temperature, the same morphology was obtained all along the substrate. For example, no significant variation was observed in the columnar grain size. As described in reference [13], at 623 K, divergent polycrystalline sheaths are formed, each composed of several

columnar single crystals. At 753 K, the "columns" are composed of individual straight-sided single crystals.

The presence of particles in the layer is to be expected at higher temperatures [6] but is barely observed between 573 and 753 K. Furthermore, the reaction rate in the gas phase do not lead to a complete consumption of reactants and deposition occurs at significant rates.

It must be noticed here that no precautions were observed to handle water. This was not necessary as it is explained just below.

The reaction of water with metal chlorides occurs only in a narrow range of temperature [573 K-753 K]. Two conditions seem to be required. First, particles formed in the gas phase must be small enough to be removed by the gas flow without being incorporated in the film during the deposition process. Particles were probably produced at a rate that prevents their agglomeration during their residence time in the reactor. Second, the depletion of reactants by consumption in the gas phase must not be complete. This condition is probably satisfied because the gas phase reaction rate is probably slow compared to that at 1223 K [6]. The fact that the water vapor is highly diluted in argon also helps to moderate and control this gas phase reaction rate. This indicates that films with highly satisfactory characteristics could be obtained with the use of simple hydrolysis between 573 K and 753 K, under precisely controlled conditions. That is the reason why no care was taken to handle water. The control of film uniformity depends only on the hydrodynamics of the gas flow and can be improved with the aid of modeling. Therefore, the partial pressure of water must be known.

Indeed, the oxidizing mixture contains H_2O. The highest deposition rates were obtained for a ratio of flow rates $H_2/O_2=2$ [13]. Species in the plasma are dissociated and recombine in the post-discharge to synthesise water. The partial pressure of water was determined by mass spectrometry measurements. Quadrupole Mass Spectrometry (QMS) measurements were carried out with a Balzers QMG-511 apparatus. The gas was sampled at about 50 cm from the discharge gap This distance and the diameter of the delivery line to the QMS chamber were chosen to give equal residence times for each species between the sampling point and either the substrate or the mass spectrometer chamber. The partial pressures measured in the RPECVD process by mass spectrometry thus corresponded to those existing in the upstream region of the substrate. In these conditions, the intensity of the H_2O peak (AMU=18) was noted. In a second step, experiments were carried out without plasma but with an $Ar-H_2O$ mixture. In order to control the water vapor flowrate in the reactor, two argon streams were used. The first stream carried H_2O from the saturator vessel held at 298 K, at a low gas velocity to ensure saturation of the argon by water vapor, while the second stream was adjusted to fix the total flow rate. It was possible in this way to choose the overall flow rate of argon in the system, keeping the hydrodynamic characteristics constant between the RPECVD and hydrolysis reactors. The water vapor partial pressure was thus determined by the respective flowrates in the two argon streams and was measured by quadrupole mass spectrometry. The flowrates of the two argon streams were adjusted so that the H_2O signal from the mass spectrometer was identical to that measured in the RPECVD process. The H_2O peak intensity was found to be equal to that measured with the post-discharge when the argon flowrates were 15 sccm for the water-carrying gas and 1000 sccm in the discharge tube.

It can be concluded that the use of a plasma here helps only in synthesizing a partial pressure of water. A complete discussion is provided in [12].

4. Modeling

4.1. HYDRODYNAMIC MODELING. — The model used in this study is obtained by solving the conservation equations of continuity, momentum and energy. Equations are solved considering

Table II. — *Transport data.*

$\lambda_{Ar} = 3.71\ 10^{-5}\ T + 7.31 \times 10^{-3}\ W\,m^{-1}\,K^{-1}$
$\mu_{Ar} = 3.81 \times 10^{-8}\ T + 1.57 \times 10^{-5}\ kg\,m^{-1}\,s^{-1}$
$C_{p_{Ar}} = 520\ J\,kg^{-1}\,K^{-1}$
$D_{ZrCl_4-Ar} = 6 \times 10^{-5}\ T^{1.75}/P\ m^2\,s^{-1}$
$D_{H_2O-Ar} = 3 \times 10^{-4}\ T^{1\,5}/P\ m^2\,s^{-1}$

a stationary state. Pressure in the system is assumed large enough to consider the gas phase as satisfying the conservation equations in a continuum medium (Kn = 2×10^{-3}). The set of partial differential equations which expresses the conservation of component i (what leads to the continuity equation by summing over i), the momentum and energy balance is closed by the ideal gas law:

$$\nabla \cdot (\rho\omega_i \mathbf{v} - D_i \rho \nabla\omega_i) = S_{\omega i} \tag{1}$$

$$\nabla \cdot \rho\mathbf{v}\mathbf{v} - \nabla \cdot \overline{\overline{\tau}} = -\nabla \mathrm{P} + \rho\mathbf{g} \tag{2}$$

$$\nabla \cdot (\rho C_p T\mathbf{v} - k\nabla T) = S_T \tag{3}$$

ρ is the fluid density; $\mathbf{v}$ the velocity; ω_i the mass fraction and S_{ω_i} is the consumption source of the reactive species (the deposition kinetics) as specified further. The species balance (1) can be solved to yield the mass fraction fields. Each reactive species is assumed to be dilute in argon, allowing for the use of a simple form of Fick's law. D_i is then considered as the binary diffusion coefficient in argon.

$\overline{\overline{\tau}}$ is the stress tensor. $\rho\mathbf{g}$, T, P, C_p and k are respectively the gravitation force, fluid temperature, pressure, specific heat at constant pressure and thermal conductivity. S_T are heat sources and are taken here equal to 0. The flow is assumed to be laminar (Re=20). Convection regime is forced ($Gr/Re^2=10^{-3}$). Heat viscous dissipation is neglected. Soret and pressure diffusions, Dufour effect, gas radiation absorbance likewise are herein ignored. All the transport data are given in Table II.

Many works on CVD modeling were carried out by taking into account very complex chemistry and transport phenomena [14–30]. It was impossible to develop a very sharp modeling of the $Ar-H_2O-ZrCl_4$ system. Most of the data required are not available to take into account specific phenomena like those neglected. A dilute medium is the key parameter of the excellent control of the process.

4.2. Kinetics Model. — In a previous paper [12], a study of the possible reaction pathways that can lead to the deposition of the ZrO_2 films establishes that, in the range [573 K-753 K], the main reaction leading to zirconia formation was:

$$ZrCl_4 + 2H_2O \rightarrow ZrO_2 + 4HCl.$$

This reaction pathway was applied to the heterogeneous reaction. It is also applied to gas phase reaction but with a different rate constant. This is necessary to take into account the reactant depletion due to the gas phase consumption. It is observed that in the RPECVD process, hardly no particle formed in the gas phase falls onto the film. It is known [11] that at high temperature (1223 K), unsuitable results are obtained when water reacts with a chloride. This is due to the violent reaction between these two species which leads to particle formation and reactant consumption. Between 623 K and 753 K, particle size is probably smaller because

the reaction rate is less fast and because the particles do not agglomerate while they stay in the furnace. These small size particles are carried away by the gas flow. The depletion due to the consumption of the reactive species in gas phase is weak enough to ensure a deposition rate of a few micrometer per hour. Nevertheless, this depletion is not negligible. Indeed, this phenomenon explains how the deposition rate on the substrate can remain constant with a temperature change of 130 K as it will be presented hereafter.

Therefore, two simple coupled chemical reactions are assumed for consumption of gaseous precursors. The aim of this approach [31] is to provide rate constants for $ZrCl_4$ hydrolysis in order to predict accurate growth rates, as far as the hypotheses are concerned, under various conditions. Only direct kinetic constants are considered, by-products reaction order chosen equal to zero.

For easier notation, gas phase and surface reactions can be written as follows:

$$\mathrm{A} + 2\mathrm{B} \xrightarrow{k_{\mathrm{s,v}}} \mathrm{F} + \mathrm{P} \tag{4}$$

where A=$ZrCl_4$, B=H_2O, F = ZrO_2 and $k_{\mathrm{s,v}}$ is the rate constant for surface or gas phase reaction. The source terms of equations of continuity for A and B are therefore due to the gas phase consumption:

$$\begin{aligned} S_{\omega_\mathrm{A}} &= -k_\mathrm{v}\rho\omega_\mathrm{A}\left(\frac{\rho\omega_\mathrm{B}}{M_\mathrm{B}}\right)^2 \\ S_{\omega_\mathrm{B}} &= -2k_\mathrm{v}\frac{\rho\omega_\mathrm{A}}{M_\mathrm{A}}\frac{(\rho\omega_\mathrm{B})^2}{M_\mathrm{B}}. \end{aligned} \tag{5}$$

The growth rate is then defined by:

$$v_\mathrm{d} = \frac{M_{\mathrm{ZrO_2}}}{\rho_{\mathrm{ZrO_2}}}\mathbf{J}_{\mathrm{ZrCl_4}} \cdot \mathbf{n} \tag{6}$$

where $\mathbf{J}_{\mathrm{ZrCl_4}}$ is the molar flux of $ZrCl_4$ and $\mathbf{n}$, the normal to the surface.

4.3. Boundary Conditions. — The reaction rate is treated as boundary conditions. The (O z) velocity component v_z is assumed to be zero on the walls parallel to (O z) and v_y on those parallel to (O y). Azimuthal distribution of Ar−$ZrCl_4$ mixture is assumed to be uniform otherwise a 3D model would have been necessary. Furthermore, low substrate rotation ensures azimuthal deposition rate uniformity. The inlet flow rate of H_2O is taken equal to 15 sccm in the plasma conditions herein mentioned [13]. Temperatures are all measured, except for the inner and outer surfaces of the separating tube. The estimation of these temperatures has been achieved by considering the separating tube as a heat transfer exchanger wall. Then, the temperature of each side of the wall would be provided by equations (7) and (8).

$$T_{\mathrm{w_c}} = T_{\mathrm{m_c}} + h_\mathrm{g}(T_{\mathrm{m_h}} - T_{\mathrm{m_c}})/P_\mathrm{c}h_\mathrm{c} \tag{7}$$

$$T_{\mathrm{w_h}} = T_{\mathrm{m_h}} - h_\mathrm{g}(T_{\mathrm{m_h}} - T_{\mathrm{m_c}})/P_\mathrm{h}h_\mathrm{h} \tag{8}$$

where the subscript c is for the cold (inner) wall and h for the hot (outer) wall. T_m is the average temperature of each fluid and P is the perimeter The hot fluid refers to that coming from the chlorination chamber (623 K) and the cold from the plasma mixture (400 K) [32].

Each wall temperature required the calculation of h_g which is the overall heat transfer coefficient, given in [33] as:

$$\frac{1}{h_\mathrm{g}} = \frac{1}{P_\mathrm{c}h_\mathrm{c}} + \frac{\ln\left(\frac{P_\mathrm{h}}{P_\mathrm{c}}\right)}{k_{\mathrm{solid}}} + \frac{1}{P_\mathrm{h}h_\mathrm{h}}. \tag{9}$$

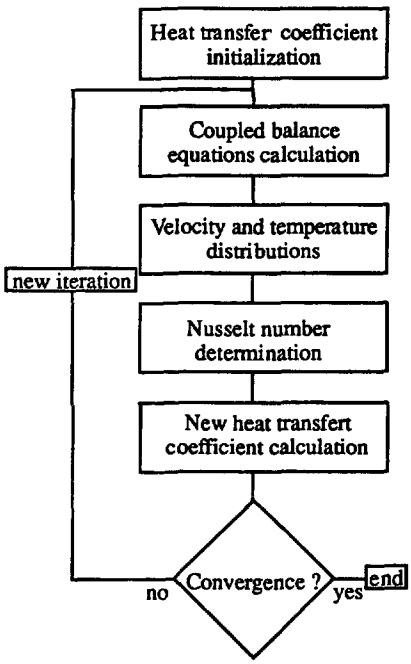

Fig. 2. — Wall temperature and heat transfer coefficient calculation algorithm.

Here k_{solid} is the thermal conductivity of the quartz tube; h_c and h_h are the heat transfer coefficients for cold and hot walls. The latter are linked to the dimensionless wall temperature gradient at each wall of the tube represented by the Nusselt number, and the gas conductivity k by equation (10):

$$h_{c,h}(z) = -k_{c,h}\left(\frac{\partial \tilde{T}(y,z)}{\partial \tilde{y}}\right)_{\tilde{y}=1} / D_{c,h} = -k_{c,h}\mathrm{Nu}(z)/D_{c,h} \tag{10}$$

where $\tilde{T}$ and $\tilde{y}$ are defined by

$$\tilde{T} = (T - T_m)/(T_w - T_m) \text{ and } \tilde{y} = y/R.$$

Therefore, the equations above can only be solved by an iterative process which is described Figure 2. When convergence is achieved, the temperatures are determined as are the heat transfer coefficients.

This approach requires no specific hypothesis on the heat exchanger wall geometry as is usually the case with the use of correlations.

4.4. Calculation Data. — Incomplete knowledge of chemical kinetics can be offset by the use of thermodynamic data [34]. With simple kinetics, involving no gas phase reaction, if deposition is known to be diffusion limited, the surface rate constant can be chosen at a sufficiently large value [35]. To solve the problem of the $ZrCl_4$–H_2O system, rate constants are estimated by the use of the modeling with experimental measurements. In order to validate their values, conditions are changed and the model compared with experimental results. Kinetic

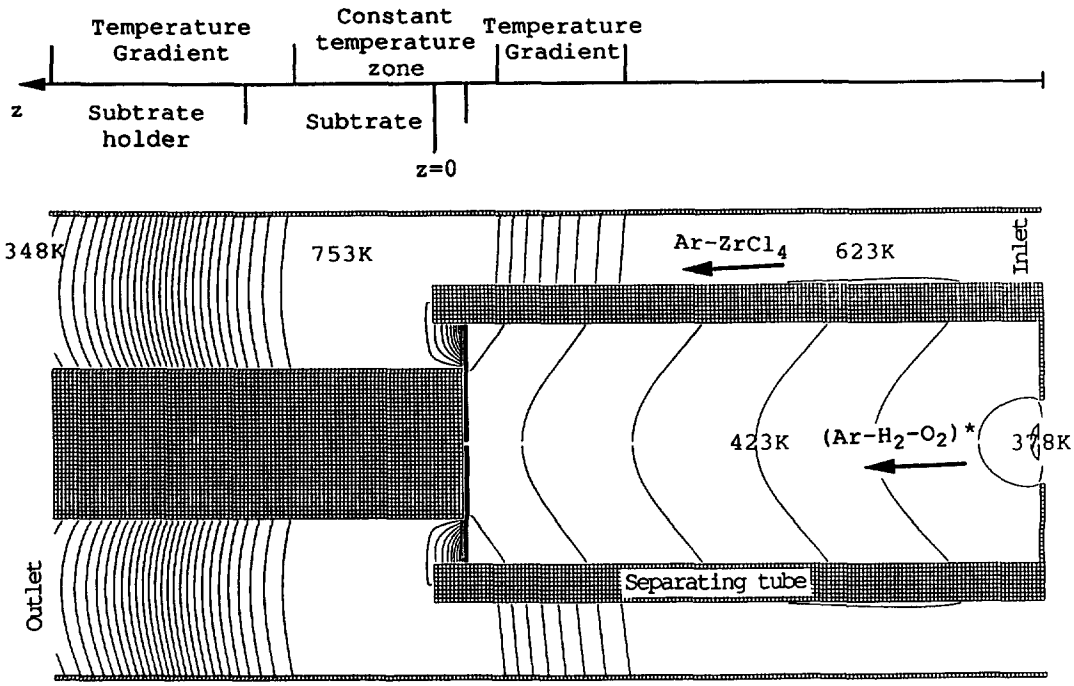

Fig. 3. — Temperature distribution at a furnace temperature of 753 K in reference conditions. Isolines are every 15 K

constants can not be considered as simple parameters whose values are adjusted to fit with the experiment results. When conditions are changing from those that are used for their estimation, the accuracy of the experiments with the modeling results is no longer due to a simple parameter adjustment.

Thermal conductivity, heat capacity and viscosity of mixtures are estimated by considering pure argon properties, assuming a very dilute medium. H_2O and $ZrCl_4$ binary diffusion coefficients in argon are estimated from calculations [36] with critical values from [36, 37].

Computational mesh is cylindrical. It is 56×250 cells in r and z directions. Dimensions of cells are 0.5×5 mm^2. Incorporating the axisymmetry assumption, the computational domain is reduced to a half of the reactor. The implicit Phoenics code is used for this calculation. Radial dimension is multiplied by a scale factor of 25 for the presentation of results (Figs. 3 to 6).

5. Results and Discussion

5.1. Temperatures and Velocities Distribution. — At a furnace temperature of 753 K, this temperature being that of the isothermal zone, temperatures distribution in the reactor is recorded in Figure 3 for the geometrical configuration where the substrate enters the separating tube. At a furnace temperature of 753 K, for outer location, temperatures are recorded in Figure 4.

The post-discharge mixture (*i.e.* the cold fluid) is heated while flowing in the separating tube. Its heating is influenced by the substrate position (Figs. 3 and 4). This substrate,

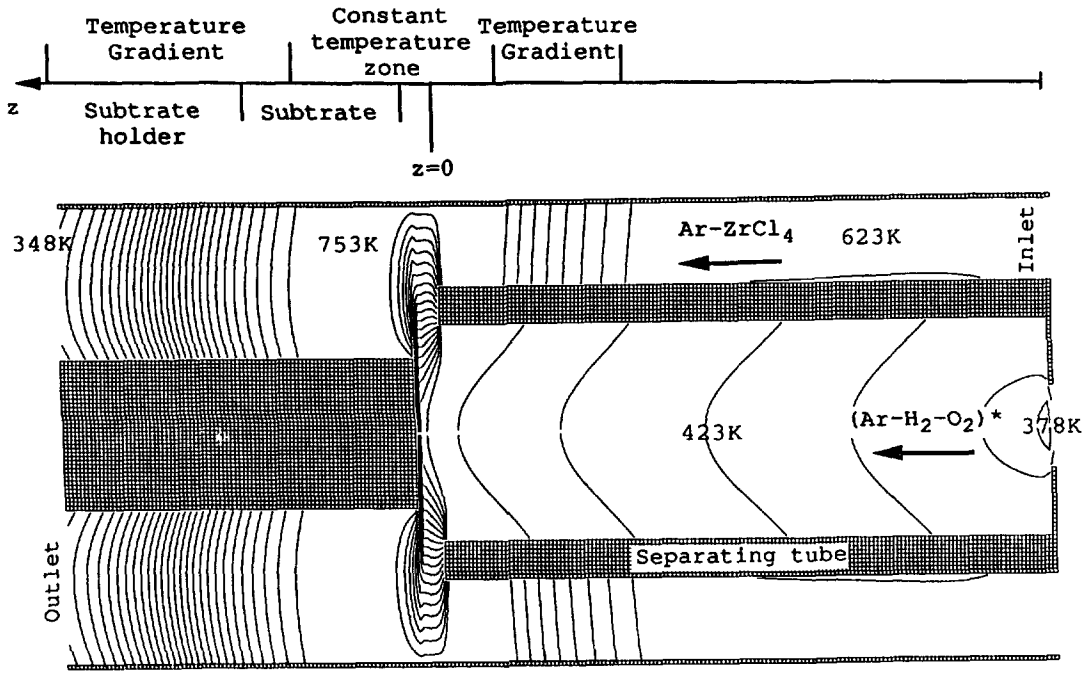

Fig. 4. — Temperature distribution at a furnace temperature of 753 K in reference conditions with the substrate located outside the separating tube. Isolines are every 15 K.

essentially heated by radiation, acts as another heating source for the gas mixture.

When the substrate is located outside the separating tube, the mixing-zone of gases is not isothermal as is nearly the case for the second configuration. When the substrate is inside, the mixing of gases is done on the substrate at constant temperature.

Calculated isotherms show that a very sharp jump is occurring at the leading edge of the substrate. This is due to the fact that the gas is heated very rapidly, while it is cold and flows on hot surfaces.

Flow is assumed to be laminar regardless of conditions (Re = 20). Diffusion in the flowing direction is negligible compared to convection ($Pe > 10$) for both $ZrCl_4$ and H_2O in the reference conditions as well as when the Ar-$ZrCl_4$ mixture velocity is increased.

In the mixing-zone of the post-discharge with gases flowing from the chlorination chamber, $ZrCl_4$ is essentially convected, in reference conditions, to the wall of the reactor. This can be observed by considering the mass fraction of $ZrCl_4$ (Fig. 5). In this figure (and also in Fig. 6), the mass fractions are given in the range [0.002, 0.02] because values outside this range are those of the parts of the reactor where no mixing occurs and therefore, where they are of little interest. The zirconium tetrachloride is highly concentrated in this zone. This effect is less important with a higher flow rate of the gases coming from the chlorination chamber.

One way to improve gas distribution is to increase argon flow rate of the Ar−$ZrCl_4$ mixture what, in turn, increases Ar−$ZrCl_4$ velocity. Figure 6 illustrates velocity distribution when Ar−$ZrCl_4$ mixture velocity is equal to that of the post-discharge mixture in the separating tube, what is obtained by using a flow rate for argon that carries $ZrCl_4$ equal to 600 sccm. The convection effect is less important but still exists due to the section reduction on the

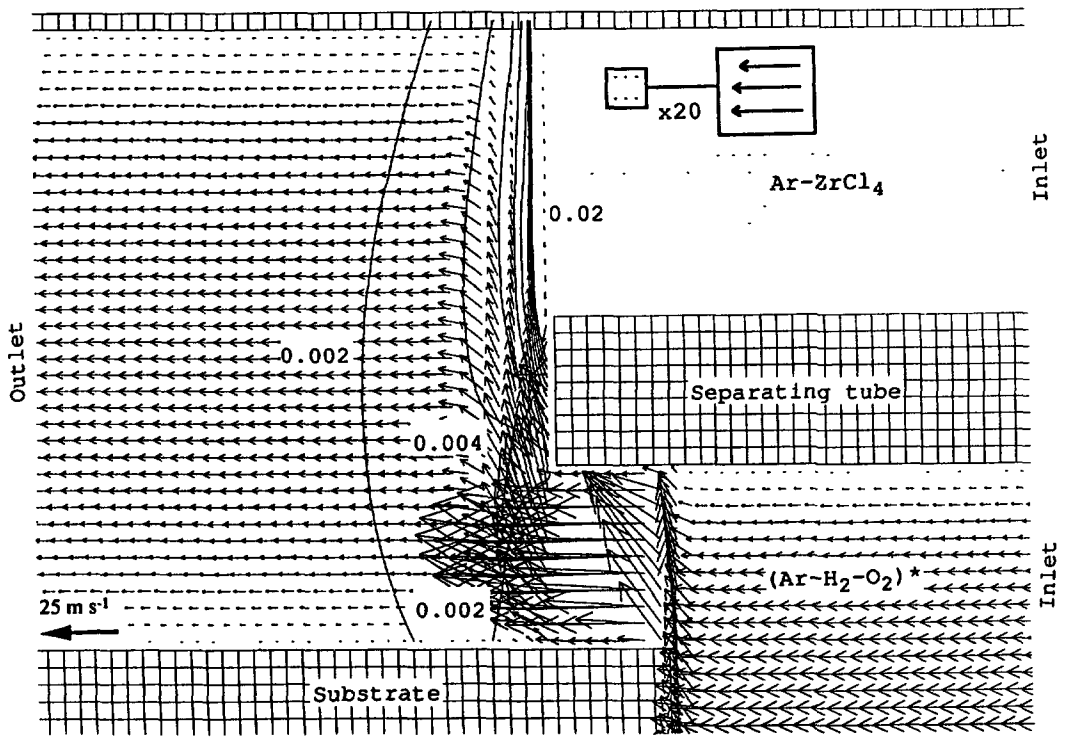

Fig. 5. — Velocity and $ZrCl_4$ mass fraction distributions in the mixing-zone of Ar-$ZrCl_4$ with the post-discharge in reference conditions (isolines are every 0.002, only values in the range [0.002-0.02] are given).

length where the substrate enters the separating tube. The main interest for disposition is to ensure a short mixing-zone of reactive species and a better uniformity of their distribution around the substrate without this mixing-volume being too extended to avoid reactive species consumption in the gas phase.

5.2. Influence of Main Process Parameters on Deposition Rate Profiles. — The first aim of this work is to calculate, *a priori*, the kinetics constants of reactions (4) and to change experimental conditions in order to validate model predictions with experimental growth rates. Calculating these constants will permit to explain the difficulties encountered by other authors on the use of water at high temperature. Each constant is calculated with an Arrhenius law:

$$k_{s,v} = k^0_{s,v} \exp(-E_{s,v}/RT)$$

The fitting is done for two temperatures of the furnace (*i.e.* 623 and 753 K) (Fig. 7). Indeed, only two temperatures are required to determine k_s and k_v which are coupled.

The best fit is obtained with:

$$k^0_s = 2.71 \times 10^{11}\ \text{m}^6\ \text{mol}^{-2}\ \text{s}^{-1}, \quad E_s = 40\ 810\ \text{J mol}^{-1}$$
$$k^0_v = 1.32 \times 10^{13}\ \text{m}^6\ \text{mol}^{-2}\ \text{s}^{-1}, \quad E_v = 88\ 570\ \text{J mol}^{-1}$$

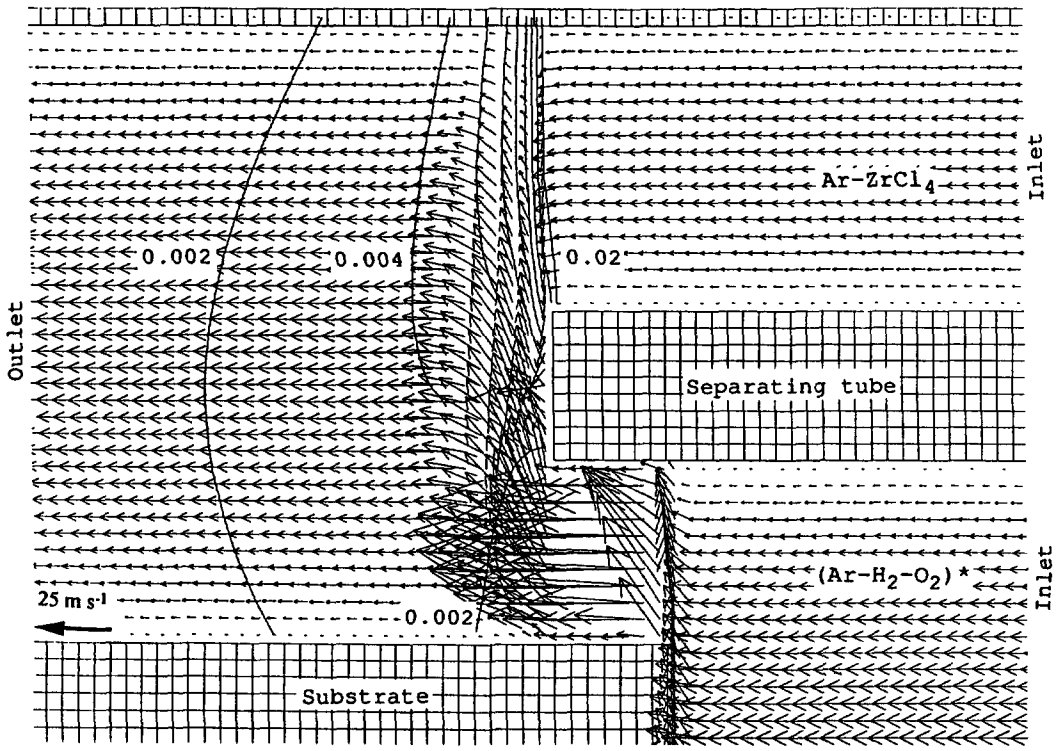

Fig. 6. — Velocity and $ZrCl_4$ mass fraction distributions in the mixing-zone of $Ar-ZrCl_4$ with the post-discharge in the separating tube with a flow rate of carrying $ZrCl_4$ argon increased to 600 sccm (isolines are every 0.002, only values in the range [0.002-0.02] are given).

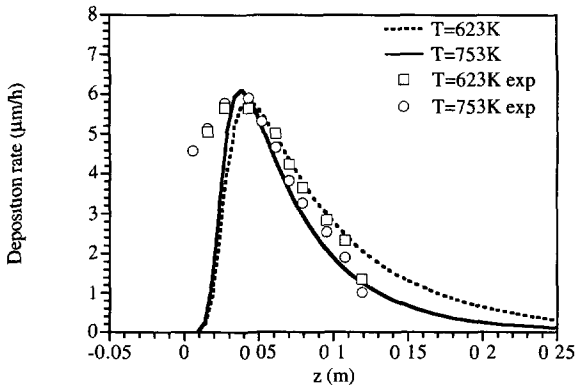

Fig. 7. — Experimental and calculated deposition rates *versus* location on the substrate in reference conditions at 623 K and 753 K.

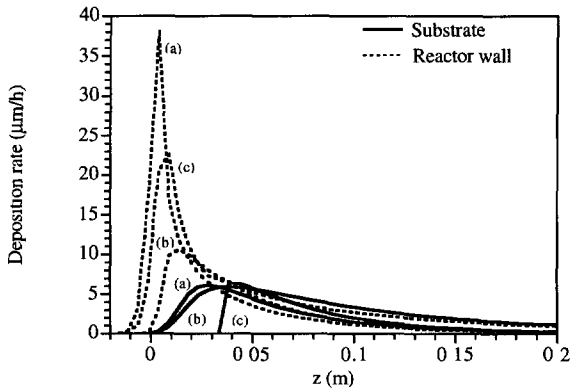

Fig. 8. — Calculated deposition rates *versus* location on the substrate (dashed lines) and on the reactor tube (solid lines), a) in reference conditions, b) when the carrying $ZrCl_4$ argon flow rate is increased to 600 sccm, c) when the substrate is located outside the separating tube.

These values were determined in a large range of values. k_s^0 and k_v^0 were investigated in the range [0, 10^{15} m^6 mol^{-2} s^{-1}] whereas E_s and E_v were investigated in the rage [0, 10^5 J mol^{-1}]. It was necessary to choose k_v different from 0. This was necessary because the only way to explain that the deposition rate remains constant while temperature of the furnace decreases by 130 K is to introduce a gas phase reaction. Indeed, if one assumes that the reaction leading to zirconia formation at the wall is unchanged, this means that the reaction is not thermally activated. It is well known that the hydrolysis of $ZrCl_4$ at 900 K is so violent that the process can not be controlled. Furthermore, particles incorporated in the films were a few but their presence proves that the gas phase reaction is possible.

The accuracy of the presented rate constants is hard to define. Indeed, these values depend on the choice made for $ZrCl_4$ transport properties (diffusion coefficient, thermal coefficient and viscosity) and on the deposition mechanism (the reaction order was assumed to be equal to 2). First, $ZrCl_4$ transport data are not known exactly. Secondly, the above values are capable of integrating several elementary processes and are only representative of an overall mechanism.

For a given k_v, changing the values of k_s of 10% for example leads to a decrease or an increase of the maximum calculated deposition rate by 10% also, the general shape of the curve being weakly changed. Changing k_v modifies the deposition rates so that they do not superimpose any longer when varying the temperature. Therefore, the rate constants lead to satisfying modeling results for values that can be weakly different from those proposed above.

The experimental values of deposition rates at 623 K and 753 K are nearly identical (Fig. 7). Both curves exhibit a maximum. The ascending part of the profiles is due to the mixing of Ar-$ZrCl_4$ with Ar−H_2O. The descending part is conversely due to reactive species consumption. On the reactor wall (Fig. 8), ZrO_2 deposition rate has the same shape but demonstrates a higher maximum rate. The difference of both rates can be explained by the convection effect due to velocity difference between Ar−$ZrCl_4$ and Ar−H_2−O_2, as shown in Figure 6. Up to the present, deposition rates on the reactor wall are not measured due to the azimuthal heterogeneity of gases distribution that leads to non constant deposition rates.

The only way to explain deposition rate remaining constant while the temperature of the furnace decreases by 130 K is by gas phase reaction. Deposition rate depends on temperature, but also on reactive species concentration. Therefore, effect of kinetic constant decrease (due to lower temperatures) can be explained by concentration increase (due to lower gas phase

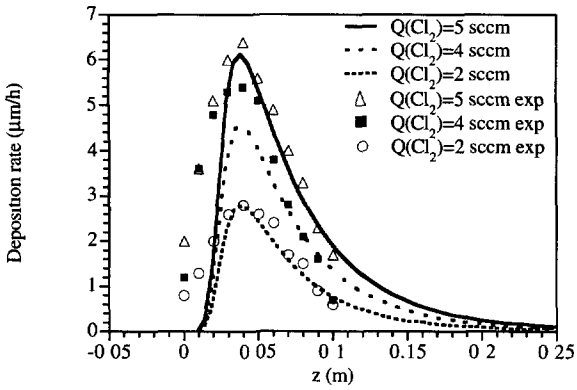

Fig. 9. — Experimental (blobs) and calculated (solid lines) deposition rates *versus* location on the substrate in reference conditions for different chlorine flow rates (circles: 2 sccm, diamonds: 4 sccm, triangles: 5 sccm).

consumption) leading to constant or decreasing [38] deposition rate profiles.

It could be imagine that the gas phase reaction is highly thermally activated and that the surface reaction is not or very little thermally activated. In this case, the gas phase reaction should have a negligible reaction rate at 573-753 K. It is assumed here that this is not the case despite no matter balance could be done. This was not possible because of the very little diameter of the particles synthesized in the gas phase. But we have noticed that a large amount of hydrolysed zirconia could be found at the end of each experiment in the pumping group.

Nonetheless, a higher volume activation energy than that for surface was found. Two highly activated reactions are concluded. This is what was looked after. Indeed, these high values explain that at high temperature, the hydrolysis of $ZrCl_4$ becomes extremely violent and leads to unsuitable results because a lot of particles are formed in the gas phase. It can be concluded from the previous quantitative study that the control of this reaction can only be ensured by the use of very diluted species in argon. In order to avoid a complete depletion of the reactive species by consumption in the gas phase, the reaction rate increase due to the constant increase with the temperature must be offset by the decrease of the partial pressure of $ZrCl_4$ and H_2O.

Deposition rates, obtained at two temperatures of the uniformly heated zone, were used to calculate unknown kinetic constants. The validation is provided in changing parameters of the process which do not affect plasma characteristics (*i.e.* Cl_2 flow rate, argon flow rate of the $Ar-ZrCl_4$ mixture and substrate location). The higher the Cl_2 flow rate, the higher the deposition rate (Fig. 9).

5.3. Improvement of the Deposition Rate Homogeneity. — To improve length deposition rate homogeneity, an additive argon flow is introduced outside the chlorination chamber to increase the velocities of the $Ar-ZrCl_4$ without affecting the chlorination reaction yield. Temperature decrease also leads, in theory, to constant deposition rate, when surface reaction becomes rate limiting, but the structure of the layer is changed. Increasing the flow rate of argon in the $Ar-ZrCl_4$ mixture is also preferred to $ZrCl_4$ flow rate increase because calculations have demonstrated that very high chlorine flow rates should be used to reach constant deposition rate. When the flow rate of argon carrying $ZrCl_4$ is increased, the deposition profile is flattened and the maximum position is shifted with rate remaining essentially unchanged (Fig. 10). The flow rate of argon carrying $ZrCl_4$ is increased, which implies a dilution effect

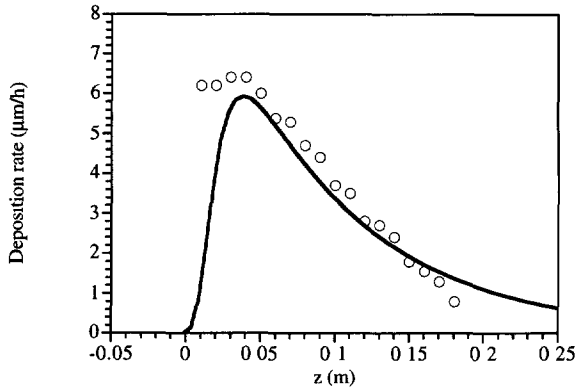

Fig. 10. — Experimental (blobs) and calculated (solid lines) deposition rates *versus* location on the substrate in reference conditions with the carrying $ZrCl_4$ argon flow rate increased to 600 sccm.

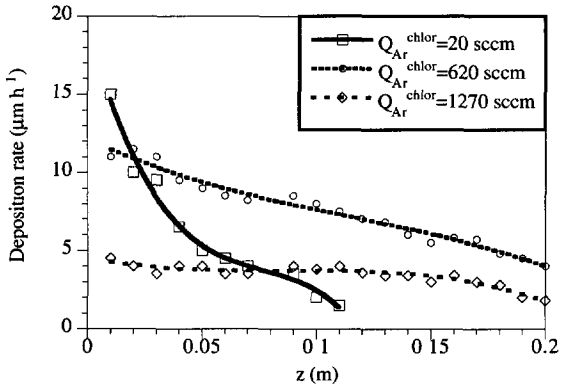

Fig. 11. — Experimental deposition rates *versus* location on the substrate with the carrying $ZrCl_4$ argon flow rate increased to 1270 sccm. The substrate was in contact in this case with the separating tube.

but also results in a better distribution of $ZrCl_4$. This can be seen by comparing the ratio of the maximum deposition rate on the wall of the reactor with the maximum deposition rate on the substrate (Fig. 8). This ratio is equal to 6.3 in reference conditions and 1.7 when the substrate is located outside the separating tube. This demonstrates that $ZrCl_4$, convected to the reactor wall when argon flow rate is low, is available to react on the substrate, which offsets the dilution effect to give an almost constant deposition rate.

In the experimental configurations studied, flat profiles could not be obtained with flow rates below 1400 sccm, *i.e.* the maximal flow rate available with the mass flow meters used here. New experiments were carried out by changing the position of the substrate holder axe. It was moved so that the substrate was in contact with the separating tube inner wall. The diffusion distance for $ZrCl_4$ was therefore shortened and the deposition rate increased. In these conditions, results presented in Figure 11 were obtained. Flat profiles could be obtained over 20 cm. Increasing the flow rate of argon carrying $ZrCl_4$ leads to a decrease of the deposition rate due to the dilution effect. Qualitatively, the same results were obtained when the power delivered to the plasma decreased from 130 to 20 W [13]. The results could not be obtained

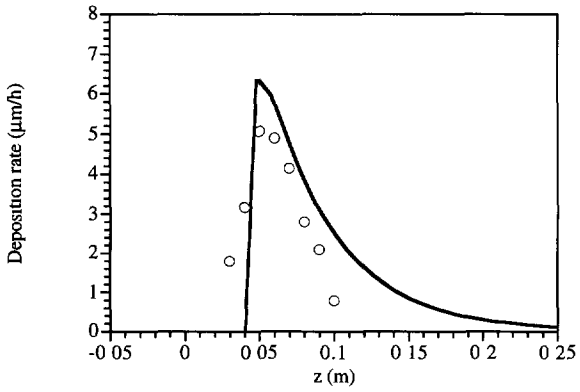

Fig 12. — Experimental (blobs) and calculated (solid lines) deposition rates *versus* location on the substrate in reference conditions, the substrate being located outside the separating tube.

by calculation because a 3D modeling would have been necessary.

When substrate is removed from the separating tube, gas distribution is improved when compared with reference conditions. The ratio introduced above is then equal to 3.7. Thus, the influence of the short zone where the section is diminished while the substrate is entering the separating tube, is determined.

Substrate location also notably influences deposition rate profiles. When the substrate is located inside the separating tube, the mixing of both gases occurs right on-side the substrate, what results in the ascending part of the profile whereas for external configuration, the mixing has already occurred when gases encounter the substrate and deposition profile demonstrates a shortened ascending part and is only slightly decreasing (Fig. 12). Deposition rate is only weakly diminished in the former case. This lower maximum rate can be attributed to lower temperatures of the mixing-zone when the substrate is out of the separating tube. Gas phase consumption is therefore reduced and mixing-zone length depends mainly on gas velocity.

It can be pointed out that the hydrodynamic conditions leading to zirconia formation are very precise. The consumption of the reactive species in the gas phase must not be too high. Powders size must remain low while they flow in the reactor to be evacuated. These conditions depend on the kinetics of $ZrCl_4$ hydrolysis which is controlled by the temperature and by the partial pressures of water and zirconium tetrachloride. The temperature effect on the reaction kinetics is determined with this work. The partial pressures of the reactive species have to be low enough between 573 K and 753 K to ensure a reproducible control of the deposition process. This is probably for these reasons that zirconia synthesis in this range of temperature is ensured, in all the examples available in the literature, by non conventional CVD processes.

6. Conclusion

A 2D hydrodynamic and chemical model of a flowing post-discharge enhanced chemical vapor deposition is provided for given plasma parameters. This approach is very useful in its ability to study a simple macroscopic deposition mechanism. Consumption of reactive species by gas phase reaction is taken into account. The rate constants for zirconium tetrachloride hydrolysis are proposed for gas phase and surface reactions. This also helps us in understanding, under given plasma conditions, transport phenomena and the influence of parameters which do not affect plasma characteristics. The gas distribution and deposition rate homogeneity over length

are improved by increasing the velocity of argon in the $Ar-ZrCl_4$ mixture. Substrate location is also found to play a important part on the deposition rate profiles.

These findings should stimulate future work that will focus on plasma analysis to link plasma processes with transport phenomena and water synthesis. The future discussion of rate controlling steps involved in the process should also be considered.

Acknowledgments

Fragema is gratefully acknowledged for its support of this work.

References

[1] Ortiz A., Falcony C., Faria M., Cota-Araiza L. and Soto G., *Thin Solid Films* **6** (1991) 206.
[2] Lucovsky G., Tsu D.V., Rudder R.A. and Markunas R.J., Thin Film Processes II, J.L. Vossen & W Kern Eds. (Academic Press inc. 565, 1991).
[3] Lösl J., Arendt R., Tamme M., Bielan S., Paduschek P., Kulish W., Kassing R., Frenck H.F. and Trier F., Proc. 10th International Symposium on Plasma Chemistry, U. Ehlemann H.G. Lergon K. Eds. (Wiesemann Bochum Germany 2.4-2pl, 1991).
[4] Dalal V.L., Leonard M. and Balwin G., *J. of Non-Crystalline Solids* **71** (1993) 164.
[5] Favia P., Caramia A., de Santis C., Colaprico V. and d'Agostino R., Proc. 10th International Symposium on Plasma Chemistry, U. Ehlemann H.G. Lergon K. Eds. (Wiesemann Bochum Germany, 2.3-1, 1991) p. 1.
[6] Meikle S., Nomura H., Nakanishi Y. and Hatanaka Y., *J. Appl. Phys.* **67** (1990) 483.
[7] Kushner M.J , *J. Appl. Phys.* **71** (1992) 4173.
[8] Kim E.T. and Yoon S.G., *Thin Solid Films* **227** (1991) 7.
[9] Seiberras G., Indrigo C., Rousseau V., Leprince P. and Mevrel R., Conférence Internationale sur les Plasmas Antibes (1993) 375.
[10] Iltis X., Viennot M., David D., Hertz D. and Michel H., *J. of Nuclear Mat.* **209** (1994) 80.
[11] Brennfleck K, Fitzer E. and Mack G., Proc. CVD VIII, J.M. Blocher, G.E. Vuillard and G. Wahl Eds. (Eindhoven, 1983) p. 44.
[12] Gavillet J., Belmonte T., Hertz D. and Michel H., *Thin Solid Films* **301** 1-2 (1997) 35.
[13] Gavillet J., Hertz D., Belmonte T. and Michel H., Supplément à la revue "Le Vide, science, technique et applications" **275** (1995) 218
[14] de Croon M.H.J.M. and Giling L.J., *J. Electrochem. Soc.* **137** (1990) 2867.
[15] Kwatera A., Ceramics International **17** (1991) 11.
[16] Rhee S., Szekely J., Ilegbusi O.J., *J. Electrochem. Soc.* **134** (1987) 2552.
[17] Hartig M.J. and Kushner M.J., *J. Appl. Phys.* **62** (1993) 1594.
[18] Dew S.K., Smy T. and Brett M.J., *J. Vac. Sci. Technol. B* **10** (1992) 618.
[19] Houf W.G., Grear J.F. and Breiland W.G., *Materials Science and Engineering B* **17** (1993) 163.
[20] Schröder K.W., Schlote J. and Hinrich S., *J. Electrochem. Soc.* **138** (1991) 2466.
[21] Whitby E. and Tsuzuki K., *IEICE Trans. Electron.* **E75-C7** (1992) 852.
[22] Weber C., van Opdorp C. and de Keijser M., *J. Appl. Phys.* **67** (1990) 2109.
[23] Evans G. and Greif R., *Trans. of the ASME: J. of Heat Transfer* **109** (1987) 928.

[24] Fiotadis D.I., Boekholt M., Jensen K.F. and Richter W., *J. of Crystal Growth* **100** (1990) 577.
[25] Visser E.P., Kleijn C.R., Govers C.A.M., Hoogendoorn C.J. and Gilıng L.J., *J. of Crystal Growth* **94** (1989) 929.
[26] Roenig K.F. and Jensen K.F., *J. Electrochem. Soc.: Solıd State Scıence* **134** (1987) 1777.
[27] Brown P.W., Zhu D. and Sahai Y., First International Conference on Transport Phenomena in processing., Selcuk I Guceri Ed. (Honolulu, Hawaii, 1992) p. 113.
[28] Knuton K.L., Carr R.W., Liu W.H. and Campbell S.A., *J. of Crystal Growth* **140** (1994) 191.
[29] Theodoropoulos C., Ingle N.K., Moutziaris T.J., ChenZ-Y., Liu P.L., Kioseoglu G. and Petrou A., *J. Electrochem. Soc.* **142** (1995) 2086.
[30] de Keijser M. and Dormans G.J.M., *J. of Crystal Growth* **149** (1995) 215.
[31] Desu S.B. and Kaldindi S.R., *Japanese Journal of Applied Scıences* **29** (1990) 1310.
[32] Malvos H., thèse INPL France (1993).
[33] Poirier D.R and Geiger G.H., Transport Phenomena in Materials Processing, TMS Mınerals Metals Materials Ed. (1994).
[34] Pons M., Bernard C. and Madar R., *Surface and Coatıngs Technology* **61** (1993) 274.
[35] Pons M., Klein R., Arena C. and Mariaux S., *J. Phys. Coll. France* **50** (1989) C5-57.
[36] Reid R.C. and Sherwood T K., The Properties of Gases and Liquids Ed. (Mc Graw Hill Inc., Second edition, 1966).
[37] Janaf, Thermochemical Tables (1966).
[38] Sladek K.J., *J. Electrochem. Soc.: Solıd State Scıence* **118** (1971) 654